

STATISTICAL PROPERTIES OF GRAVITATIONAL LENSING IN COSMOLOGICAL MODELS WITH COSMOLOGICAL CONSTANT *

LEE, HYUN-A and PARK, MYEONG-GU

Department of Astronomy and Meteorology, Kyungpook National University, Taegu

(Received Jul. 27, 1994; Accepted Sep. 10, 1994)

ABSTRACT

To extend the work of Gott, Park, and Lee (1989), statistical properties of gravitational lensing in a wide variety of cosmological models involving non-zero cosmological constant is investigated, using the redshifts of both lens and source and observed angular separation of images for gravitational lens systems. We assume singular isothermal sphere as lensing galaxy in homogenous and isotropic Friedmann-Lemaitre-Robertson-Walker universe, Schechter luminosity function, standard angular diameter distance formula and other galaxy parameters used in Fukugita and Turner (1991). To find the most adequate flat cosmological model and put a limit on the value of dimensionless cosmological constant λ_0 , the mean value of the angular separation of images, probability distribution of angular separation and cumulative probability are calculated for given source and lens redshifts and compared with the observed values through several statistical methods. When there is no angular selection effect, models with highest value of λ_0 is preferred generally. When the angular selection effects are considered, the preferred model depends on the shape of the selection functions and statistical methods; yet, models with large λ_0 are preferred in general. However, the present data can not rule out any of the flat universe models with enough confidence. This approach can potentially select out best model. But at the moment, we need more data.

Key Words : gravitation, gravitational lensing, galaxy, QSO, cosmology

I. INTRODUCTION

The gravitational lensing is a phenomenon to form a variety of images. It occurs when two or more objects at different distance from the observer happen to lie along the line of sight and the light from more distant object is bent by the gravitational field of the foreground mass.

Gravitational lens images may be multiplied, distorted, or magnified(or demagnified): the formation of images depends on the relative position of source and lens, brightness distribution of the source, and mass distribution of the lens. The light source is typically a quasar or a galaxy; the lens (or deflector) is a galaxy or a cluster of galaxies.

According to Einstein's general relativity, a massive object curves spacetime, and hence bends the passing light. Since this effect depends on the shape and the strength of the gravitational field which is determined by the mass distribution of lens, we can deduce from the characteristics of images the informations of the mass distribution of lens. It is also affected by the shape of the spacetime of the universe as a whole. Hence gravitational lensing plays a very important role in understanding the structure of universe and the distribution of dark matter, believed to provide more than 90% of the total density of present universe.

The first observational evidence of the gravitational lensing was the discovery of the multiple quasar system, Q0957+561 (Walsh et al. 1979). The two quasars, whose angular separation is $6.15''$ and whose redshifts are both

* This work is in part supported by Korea Research Foundation grant 01-D-0081.

1.41, are the gravitationally lensed images of the same quasar formed by the foreground galaxy whose redshift is known to be 0.39 aided by the cluster of galaxies around it (Young et al. 1980). More gravitational lens systems have been discovered since then and now the total number of all kinds of lensing is more than 20. Among them, about 10 are multiple-image systems.

Turner, Ostriker, and Gott (1984, hereafter TOG) applied statistical analysis on multiple-image lens systems. Assuming that lensing galaxy is either a point mass or singular isothermal sphere (SIS) uniformly distributed in space, they calculated the mean angular separation of images, the distribution of lens redshift, and the probability of lensing event in standard Λ Friedmann-Robertson universe, taking into account the selection effect by flux amplification and finite angular resolution. They found that results depend more on the central velocity dispersions of bright elliptical galaxies and maximum surface densities in great clusters than on the assumed cosmology. The average separation of images is about $4.6''$, which is larger than would be expected if we observe a fair sample of lenses, and the distribution of lens redshifts shows maximum frequency around 0.5 with the large majority of cases less than 1.

Gott, Park, and Lee (1989, hereafter GPL) studied the probability of gravitational lensing and the mean separation of images in cosmological models with non-zero cosmological constant. However they did not quantitatively compare predicted values derived with observed ones due to the insufficient observational data.

Fukugita and Turner (1991, hereafter FT) calculated the number of predicted multiple images lens systems in flat universe with non-zero cosmological constant, and placed a limit on cosmological constant by comparing with the number of observed multiple images lens systems using Hewitt and Burbidge (1987, 1989) samples involving 4250 quasars and Boyle et al. (1990) samples involving 420 quasars.

Fukugita, Futamase, Kasai, and Turner (1992, hereafter FFKT) repeated similar calculations incorporating various details that were not considered in FT study. Since large cosmological constant predicted more lens systems than are observed, they concluded that the dimensionless cosmological constant, $\lambda_0 = \Lambda/3H_0^2$, is not over 0.9.

Cosmological models with non-zero cosmological constant regained some popularity recently due to several advantages. First, it is the age problem of Universe. The estimated age of old globular cluster in our galaxy is larger than that of the universe derived from Hubble constant $H_0 = 70 \sim 80 \text{ km sec}^{-1} \text{ Mpc}^{-1}$, value preferred in recent studies (Carroll et al. 1992). The contradiction can be resolved by cosmological models having non-zero cosmological constant as is well known. Second, the number of predicted galaxies in flat universe with zero cosmological constant is fewer than that of faint galaxies in recent observations (see reference in Carroll et al. 1992). Cosmological models having non-zero cosmological constant can be one of the solutions although some recent studies argue against it (Koo & Kron 1992). Third, the peculiar motions and the distribution of galaxies in large scale structure, and the fluctuation of cosmic microwave background radiation obtained from COBE observation do not agree with the model of galaxy formation in zero cosmological constant universe. So, in this paper we calculate the mean value and the probability distribution of angular separations of images in various cosmological models especially when the redshifts of source and lens are known. We compare the results with observations to find the limit on cosmological constant. In §II we explain the basics of the lens statistics and observational data. In §III we calculate the predicted mean value and the probability distribution, and the cumulative probability of the angular separation of images in the presence of the selection effects as functions of the redshift of lens and source in various cosmological models with non-zero cosmological constant. The calculated results are compared with observational data by several statistical test, including Monte-Carlo simulation test.

II. STATISTICAL PROPERTIES OF GRAVITATIONAL LENS : ASSUMPTIONS & CALCULATIONS

(a) spacetime

We adopt the Robertson-Walker universe,

$$ds^2 = dt^2 - R^2(t) \left\{ \frac{dr^2}{1 - kr^2} + r^2 d\theta^2 + r^2 \sin^2 \theta d\phi^2 \right\} \quad (1)$$

where $R(t)$ is the scale factor, k is 1, 0, and -1 for close, flat, and open universe respectively. Spherical coordinate

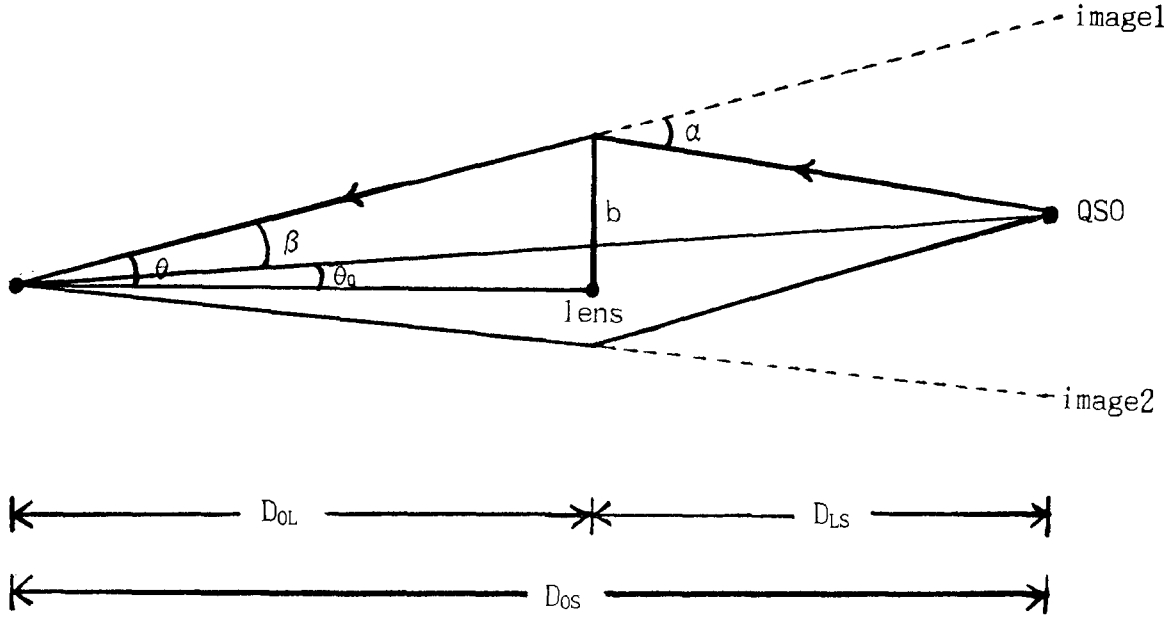


Fig. 1. Geometry of gravitational lensing and definition of symbols.
 D_{OS} : the angular diameter distance between observer and source (QSO)
 D_{LS} : the angular diameter distance between lens (galaxy) and source
 D_{OL} : the angular diameter distance between observer and lens
 β : angle between image 1 and original source position
 α : bending angle b : impact parameter
 θ : angle between lens and image 1
 θ_Q : angle between lens and original source position

(r, θ, ϕ) is a comoving coordinate which marks the position of lensing galaxies or source QSO.

(b) Gravitational lens model and lensing equations

When lens has spherically symmetric mass distribution, bending angle, α , is given by a function of impact parameter b and the mass distribution of lens $M(b)$:

$$\alpha = 4GM(b)c^{-2}b^{-1}. \tag{2}$$

We assume all lens galaxies are SIS's, whose property is characterized only by one-dimensional velocity dispersion. Albeit its simplicity, SIS is a good approximation to real mass distribution in galaxies (TOG, Maoz & Rix 1993). When bending angle is small, the gravitational lensing equation which relates the position of source, lens, and images is given by (see Figure 1)

$$D_{LS}\alpha(\theta) + D_{OS}\theta_Q = D_{OS}\theta, \tag{3}$$

where subscripts L , S , and O denote lens, source, and observer, respectively; D_{LS} is the angular diameter distance between lens and source, D_{OS} between observer and source, D_{OL} between observer and lens.

When lens is a SIS, bending angle, α , is independent of b and θ :

$$\alpha = 4\pi\left(\frac{\sigma}{c}\right)^2, \tag{4}$$

where σ is one-dimensional velocity dispersion of SIS. In this case, two images will be observed at a distance $\pm\beta_{crit}$ from the original position of QSO, and β_{crit} is given by

$$\beta_{crit} = \alpha \frac{D_{LS}}{D_{OS}} = 4\pi \left(\frac{\sigma}{c}\right)^2 \left(\frac{D_{LS}}{D_{OS}}\right). \quad (5)$$

When the source and the lensing galaxy coincide in the sky, the image becomes ‘Einstein ring’ of radius β_{crit} around the center of the lensing galaxy. When a source is within β_{crit} of the lens, two images are formed; otherwise, only one image is formed. The angular separation of two images, $\Delta\theta$, is twice of β_{crit} .

$$\Delta\theta = 2\beta_{crit} = 2\alpha \left(\frac{D_{LS}}{D_{OS}}\right) = 8\pi \left(\frac{\sigma}{c}\right)^2 \left(\frac{D_{LS}}{D_{OS}}\right) \quad (6)$$

(c) Distance formula

There are many ways to define a distance in cosmology – parallax distance, angular diameter distance, luminosity distance, proper motion distance, etc. (see Weinberg 1972). It is the angular diameter distance that is relevant to the angular separation of images. The distance between two objects in z_1 and z_2 is (GPL, FFKT),

$$d(z_1, z_2) = \begin{cases} \frac{R_0}{(1+z_2)\sqrt{\Omega_0+\lambda_0-1}} \sin(\chi_2 - \chi_1) & \text{for } k=1; \\ \frac{R_0}{(1+z_2)}(\chi_2 - \chi_1) & \text{for } k=0; \\ \frac{R_0}{(1+z_2)\sqrt{1-\Omega_0-\lambda_0}} \sinh(\chi_2 - \chi_1) & \text{for } k=-1; \end{cases} \quad (7)$$

where $R_0 = c/H_0$ is Hubble distance, Ω_0 is mean mass density of universe. We use the notation $D_{OS} = d(0, z_S)$, $D_{LS} = d(z_L, z_S)$, $D_{OL} = d(0, z_L)$. For flat universe ($k = 0 : \Omega_0 + \lambda_0 = 1$),

$$\chi_2 - \chi_1 = \int_{z_1}^{z_2} \frac{dz}{\sqrt{\Omega_0(1+z)^3 + (1-\Omega_0)}} \quad (8)$$

and for $\lambda_0 = 0$,

$$d(z_1, z_2) = \frac{2R_0\{(2-\Omega_0+\Omega_0z_2)\sqrt{1+\Omega_0z_1} - (2-\Omega_0+\Omega_0z_1)\sqrt{1+\Omega_0z_2}\}}{\Omega_0^2(1+z_1)(1+z_2)^2}. \quad (9)$$

In general ($k \neq 0 : \Omega_0 + \lambda_0 \neq 1$),

$$\chi_2 - \chi_1 = \sqrt{|\Omega_0 + \lambda_0 - 1|} \int_{z_1}^{z_2} \frac{dz}{\sqrt{\Omega_0(1+z)^3 + (1-\Omega_0-\lambda_0)(1+z)^2 + \lambda_0}}. \quad (10)$$

(d) Luminosity function

When the lensing event occurs, the distribution of image separation, $\Delta\theta$, depends on the probability distribution of lens mass or, equivalently, velocity dispersion. It is thus determined by the form of the luminosity function when the relation between velocity dispersion, σ , and luminosity, L , is known. The number density of galaxies with luminosities between L and $L + dL$ can be expressed by Schechter Luminosity function

$$\Phi(L)dL = \Phi^* \left(\frac{L}{L^*}\right)^\alpha \exp\left(-\frac{L}{L^*}\right) \frac{dL}{L^*}, \quad \alpha = -1.1. \quad (11)$$

Here we consider three types of galaxies –ellipticals, spirals, lenticulars; Φ^* and L^* have corresponding values for each type. We further assume that ellipticals and lenticulars follow Faber-Jackson relation (Faber & Jackson 1976), $L \propto \sigma^4$ and spirals Tully-Fisher relation (Tully & Fisher 1977), $L \propto \sigma^{2.6}$ (FT).

(e) Probability

The critical impact parameter is the maximum distance at lens plane between lens and source which can form multiple images:

$$a_{crit} = D_{OL}\beta_{crit}. \quad (12)$$

So lensing cross section of a galaxy to form multiple images is given by

$$\pi a_{crit}^2 = \pi(D_{OL}\beta_{crit})^2 = \pi(D_{OL}\alpha \frac{D_{LS}}{D_{OS}})^2 = 16\pi^3 (\frac{\sigma}{c})^4 (D_{LS} \frac{D_{OL}}{D_{OS}})^2, \quad (13)$$

and the differential probability of multiple lensing event by galaxies with same velocity dispersion σ at z_L is

$$d\tau = n_0(1+z_L)^3 \pi a_{crit}^2 \frac{cdt}{dz_L} dz_L = F(1+z_L)^3 (\frac{D_{LS}}{D_{OS}} \frac{D_{OL}}{R_0})^2 \frac{1}{R_0} \frac{cdt}{dz_L} dz_L, \quad (14)$$

where

$$F = 16\pi^3 n_0 (\frac{\sigma}{c})^4 R_0^3, \quad (15)$$

and n_0 is the present density of gravitational lensing objects (GPL, FFKT). The function cdt/dz in Friedmann-Lemaitre-Robertson-Walker geometry is

$$\frac{cdt}{dz_L} = \frac{R_0}{1+z_L} \frac{1}{\sqrt{\Omega_0(1+z_L)^3 + (1-\Omega_0-\lambda_0)(1+z_L)^2 + \lambda_0}}. \quad (16)$$

If the velocity dispersion of galaxies follows the distribution which is determined by Schechter Luminosity function and Tully-Fisher or Faber-Jackson relation, the differential optical depth of lensing in traveling dz_L with the angular separation of image between $\Delta\theta$ and $\Delta\theta + d\Delta\theta$ is given by

$$\frac{d\tau_j^2}{dz_L d\Delta\theta} = A \left(\frac{1}{8\pi}\right)^{2\alpha+4} \left(\frac{c}{\sigma_j^*}\right)^{4\alpha+4} (\Delta\theta)^{2\alpha+3} \exp\left[-\left(\frac{D_{OS}}{D_{LS}}\right) \left(\frac{\Delta\theta}{8\pi}\right) \left(\frac{c}{\sigma_j^*}\right)^2\right] \quad (17)$$

for ellipticals ($j = e$) and lenticulars ($j = so$) where

$$A = 16\pi^3 n_0 R_0^3 (1+z_L^3) \left(\frac{D_{OL}}{R_0} \frac{D_{LS}}{D_{OS}}\right)^2 \frac{1}{R_0} \frac{cdt}{dz_L} \frac{2}{\Gamma(\alpha+2)} \left(\frac{D_{LS}}{D_{OS}}\right)^{2\alpha+4}, \quad (18)$$

and for spirals ($j = s$),

$$\frac{d\tau_j^2}{dz_L d\Delta\theta} = A' \left(\frac{1}{8\pi}\right)^{1.3\alpha+3.3} \left(\frac{c}{\sigma_j^*}\right)^{2.6\alpha+2.6} (\Delta\theta)^{1.3\alpha+2.3} \exp\left[-\left(\frac{D_{OS}}{D_{LS}}\right) \left(\frac{\Delta\theta}{8\pi}\right) \left(\frac{c}{\sigma_j^*}\right)^2\right]^{1.3}, \quad (19)$$

where

$$A' = 16\pi^3 n_0 R_0^3 (1+z_L^3) \left(\frac{D_{OL}}{R_0} \frac{D_{LS}}{D_{OS}}\right)^2 \frac{1}{R_0} \frac{cdt}{dz_L} \frac{2}{\Gamma(\alpha+2)} \left(\frac{D_{LS}}{D_{OS}}\right)^{1.3\alpha+3.3}. \quad (20)$$

So the effectiveness of the lensing is determined by two parameters: the characteristic number density in Schechter function, Φ_j^* , and the velocity dispersion, σ_j^* , corresponding to L_j^* galaxy. TOG and FT combined these parameters and defined F_j whose values are

$$F_j = \begin{cases} 0.019 \pm 0.008 : & \text{for } j=e \\ 0.021 \pm 0.009 : & \text{for } j=so \\ 0.007 \pm 0.002 : & \text{for } j=s. \end{cases} \quad (21)$$

FT also combined the previous works to estimate σ_j^* for each type of galaxies.

$$\sigma_j^* = \begin{cases} 276_{-24}^{+15} \text{ kmsec}^{-1} : & \text{for } j=e \\ 252_{-24}^{+15} \text{ kmsec}^{-1} : & \text{for } j=so \\ 134_{-12}^{+7} \text{ kmsec}^{-1} : & \text{for } j=s. \end{cases} \quad (22)$$

The mean angular separation of images, when double images of source at z_S are formed, is obtained by integrating the differential optical depth, allowing for three types of galaxies,

$$\langle \Delta\theta \rangle = \frac{\sum_{j=e,s,o,s} \int \frac{d^2\tau_j}{dz_L d\Delta\theta} \Delta\theta d\Delta\theta}{\sum_{j=e,s,o,s} \int \frac{d^2\tau_j}{dz_L d\Delta\theta} d\Delta\theta}. \quad (23)$$

The expected dispersion of separation around the mean value is

$$\sigma_{\Delta\theta} = \sqrt{\langle \Delta\theta^2 \rangle - \langle \Delta\theta \rangle^2} \quad (24)$$

with

$$\langle \Delta\theta^2 \rangle = \frac{\sum_{j=e,s,o,s} \int \frac{d^2\tau_j}{dz_L d\Delta\theta} \Delta\theta^2 d\Delta\theta}{\sum_{j=e,s,o,s} \int \frac{d^2\tau_j}{dz_L d\Delta\theta} d\Delta\theta}. \quad (25)$$

The normalized probability distribution of the angular separation when multiple images are formed is given by

$$\frac{dP}{d\Delta\theta} = \frac{\sum_{j=e,s,o,s} \int \frac{d^2\tau_j}{dz_L d\Delta\theta}}{\sum_{j=e,s,o,s} \int \frac{d^2\tau_j}{dz_L d\Delta\theta} d\Delta\theta}. \quad (26)$$

We also calculate its cumulative probability, the probability of lens separation being between 0 and $\Delta\theta$, by integrating

$$P(\Delta\theta) = \int_0^{\Delta\theta} \frac{dP}{d\Delta\theta'} d\Delta\theta'. \quad (27)$$

(f) Selection effect

So far, we do not consider the angular selection effects. But it is difficult to observe gravitational lens systems of multiple images having a very small angular separation because of the limit of resolving power. Since it is nearly impossible to represent the angular selection effects in real observations faithfully, we here consider two cases of highly simplified selection effects: selection effect I is the case when the gravitatioanal lens systems with the angular separation of images below $1.0''$ are not observed at all and those with the angular separation of images over $1.0''$ are completely observed; We take an arbitrary, yet reasonable, value of $1.0''$, partly because in reality this value changes from survey to survey. selection effect II is the one used in TOG with no detection below $0.8''$ and complete detection above $3.0''$ (refer Table 2 of TOG). These selection effects are incorporated into the probability distributions and other values derived from it: the only change is multiplying these functions to $\frac{dP}{dz_L dz_Q}$.

(g) Cosmological models

Since flat universe has more merits, we focus on the flat universe with $\Omega_0 + \lambda_0 = 1.0$ and use six cosmological models with or without cosmological constant. However, we also include an open universe for comparison.

$$\left\{ \begin{array}{lll} \text{Model (A):} & \Omega_0 = 1.0, \lambda_0 = 0.0 & \text{flat universe} \\ \text{Model (B):} & \Omega_0 = 0.5, \lambda_0 = 0.5 & \text{flat universe} \\ \text{Model (C):} & \Omega_0 = 0.2, \lambda_0 = 0.8 & \text{flat universe} \\ \text{Model (D):} & \Omega_0 = 0.1, \lambda_0 = 0.9 & \text{flat universe} \\ \text{Model (E):} & \Omega_0 = 0.0, \lambda_0 = 1.0 & \text{flat universe} \\ \text{Model (F):} & \Omega_0 = 0.1, \lambda_0 = 0.0 & \text{open universe} \end{array} \right. \quad (28)$$

Table 1. $z_L, z_S, \Delta\theta_{obs}$ for five gravitational lens systems

Name	z_L	z_S	$\Delta\theta_{obs}$
3C324	0.84	1.21	2.0
Q2237+0305	0.04	1.69	1.8
Q0142-100	0.49	2.72	2.2
MG1654+134	0.25	1.74	2.1
H1413+117	1.44	2.55	1.1

(h) Observed lens systems

In this paper, we adopt as comparison data only those lens systems to which our theoretical calculations can apply: it is very important to use the appropriate observational data, especially because there are only handful of multiple-image lens systems. The lenses (deflector) of these systems – 3C324, Q2237+0305, Q0142-100, MG1654+134 and H1413+117– are all single galaxy, and the redshifts of both lens and source are known (see Table 1). Though there are other lens systems having multiple images, we exclude other systems for various reasons: lens is not a single galaxy (e.g., Q0957+561, Q2061+112); or lens isn't observed (e.g., Q0414+053); or the redshift of the lens isn't determined (e.g., Q1115+080).

III. RESULT AND DISCUSSIONS

Using the methods explained in §II, we calculate the predicted angular separation of images and compare with the observed lens systems, considering three different selection effects.

(a) Calculation and Test Result

i) The mean angular separation of images

To probe the statistical properties of the distribution of the image separation, we calculate the expected value of the angular separation, $\langle\Delta\theta\rangle_{pred}$ by averaging $\Delta\theta$ over the probability distribution for given z_L and z_S . The results are shown in Table 2. When selection effect is not considered (no selection effect), larger λ_0 produces greater $\langle\Delta\theta\rangle_{pred}$. However $\langle\Delta\theta\rangle_{pred}$ is generally less than $\Delta\theta_{obs}$ irrespective of cosmological models considered. For selection effect I, $\langle\Delta\theta\rangle_{pred}$ is 1.2 ~ 2.1 times greater than that for no selection effect, and hence closer to $\Delta\theta_{obs}$. For selection effect II, $\langle\Delta\theta\rangle_{pred}$ is 1.4 ~ 2.2 times greater than for no selection effect, and in many cases larger than $\Delta\theta_{obs}$. In general, the value of $\langle\Delta\theta\rangle_{pred}$ increases as λ_0 increases irrespective of selection effects (see Figure 2). But for Q2237 + 0305 whose lens is close to the observer, the variation of mean angular separation of images is the least as the cosmological constant increases. The reason is that the mean angular separation of images is given as a function of D_{LS}/D_{OS} and its value is little changed through out the models.

ii) Chi-square test

To assess the statistical significance of the difference between the observed value and the predicted one, we apply chi-square test. The reduced chi-square is defined as

$$\chi^2_\nu = \frac{1}{N-1} \sum_{i=1}^N \left[\frac{(\Delta\theta_{obs})_i - \langle\Delta\theta\rangle_{pred,i}}{\sigma_{\Delta\theta,i}} \right]^2, \quad (29)$$

where N is the number of gravitational lens, $\sigma_{\Delta\theta,i}$ is the dispersion of the angular separation of images. The chi-square value and the probability are shown in Table 3.

For no selection effect and selection effect I, the probability become greater as λ_0 increases, and particularly the model (E) with $\lambda_0 = 1.0$ has the largest probability. On the other hand, for selection effect II, the models (C) and (D) with $\lambda_0 = 0.8$ and $\lambda_0 = 0.9$ have larger probabilities. For no selection effect, the models (A), (B), and (F) all of which have λ_0 less than 0.5 are rejected with 95% confidence. But for the selection effect I and II, there are no

Table 2. $\Delta\theta_{obs}, D_{LS}/D_{OS}, \langle\Delta\theta\rangle_{pred}, \sigma_{\Delta\theta, pred}$
for five gravitational lens systems

1. Model(A) : $\Omega_0 = 1.0, \lambda_0 = 0.0$ (flat universe)

Name	$\Delta\theta_{obs}$	D_{LS}/D_{OS}	$\langle\Delta\theta\rangle_{no\ sel} (\sigma)$	$\langle\Delta\theta\rangle_{sel\ I} (\sigma)$	$\langle\Delta\theta\rangle_{sel\ II} (\sigma)$
3C324	2.0	0.197	0.61(0.37)	1.25(0.27)	1.31(0.37)
Q2237+0305	1.8	0.950	1.23(0.79)	1.77(0.68)	2.41(0.81)
Q0142-100	2.2	0.625	1.94(1.19)	2.37(1.04)	3.07(0.99)
MG1654+134	2.1	0.730	2.26(1.38)	2.67(1.24)	3.38(1.15)
H1413+117	1.1	0.233	0.72(0.44)	1.33(0.32)	1.50(0.44)

2. Model(B) : $\Omega_0 = 0.5, \lambda_0 = 0.5$ (flat universe)

Name	$\Delta\theta_{obs}$	D_{LS}/D_{OS}	$\langle\Delta\theta\rangle_{no\ sel} (\sigma)$	$\langle\Delta\theta\rangle_{sel\ I} (\sigma)$	$\langle\Delta\theta\rangle_{sel\ II} (\sigma)$
3C324	2.0	0.218	0.68(0.41)	1.29(0.30)	1.42(0.41)
Q2237+0305	1.8	0.959	1.24(0.80)	1.78(0.69)	2.42(0.82)
Q0142-100	2.2	0.665	2.06(1.26)	2.48(1.11)	3.19(1.05)
MG1654+134	2.1	0.764	2.37(1.45)	2.76(1.31)	3.47(1.21)
H1413+117	1.1	0.254	0.79(0.48)	1.30(0.35)	1.61(0.49)

3. Model(C) : $\Omega_0 = 0.2, \lambda_0 = 0.8$ (flat universe)

Name	$\Delta\theta_{obs}$	D_{LS}/D_{OS}	$\langle\Delta\theta\rangle_{no\ sel} (\sigma)$	$\langle\Delta\theta\rangle_{sel\ I} (\sigma)$	$\langle\Delta\theta\rangle_{sel\ II} (\sigma)$
3C324	2.0	0.248	0.77(0.47)	1.37(0.34)	1.58(0.48)
Q2237+0305	1.8	0.967	1.25(0.81)	1.79(0.70)	2.43(0.82)
Q0142-100	2.2	0.717	2.22(1.36)	2.63(1.22)	3.34(1.13)
MG1654+134	2.1	0.801	2.48(1.52)	2.87(1.38)	3.58(1.27)
H1413+117	1.1	0.296	0.93(0.56)	1.48(0.42)	1.83(0.56)

4. Model(D) : $\Omega_0 = 0.1, \lambda_0 = 0.9$ (flat universe)

Name	$\Delta\theta_{obs}$	D_{LS}/D_{OS}	$\langle\Delta\theta\rangle_{no\ sel} (\sigma)$	$\langle\Delta\theta\rangle_{sel\ I} (\sigma)$	$\langle\Delta\theta\rangle_{sel\ II} (\sigma)$
3C324	2.0	0.268	0.83(0.51)	1.41(0.37)	1.68(0.51)
Q2237+0305	1.8	0.971	1.25(0.81)	1.79(0.70)	2.44(0.82)
Q0142-100	2.2	0.749	2.32(1.42)	2.72(1.28)	3.43(1.18)
MG1654+134	2.1	0.821	2.54(1.55)	2.93(1.41)	3.63(1.30)
H1413+117	1.1	0.329	1.02(0.62)	1.57(0.48)	1.99(0.61)

5. Model(E) : $\Omega_0 = 0.0, \lambda_0 = 1.0$ (flat universe)

Name	$\Delta\theta_{obs}$	D_{LS}/D_{OS}	$\langle\Delta\theta\rangle_{no\ sel} (\sigma)$	$\langle\Delta\theta\rangle_{sel\ I} (\sigma)$	$\langle\Delta\theta\rangle_{sel\ II} (\sigma)$
3C324	2.0	0.306	0.95(0.58)	1.51(0.44)	1.88(0.58)
Q2237+0305	1.8	0.976	1.26(0.81)	1.80(0.70)	2.55(0.83)
Q0142-100	2.2	0.820	2.54(1.55)	2.92(1.42)	3.63(1.30)
MG1654+134	2.1	0.854	2.64(1.61)	3.02(1.48)	3.73(1.35)
H1413+117	1.1	0.435	1.35(0.83)	1.84(0.68)	2.44(0.74)

Table 2. Continued
 6. Model(F) : $\Omega_0 = 0.1, \lambda_0 = 0.0$ (open universe)

Name	$\Delta\theta_{obs}$	D_{LS}/D_{OS}	$\langle\Delta\theta\rangle_{no\ sel}(\sigma)$	$\langle\Delta\theta\rangle_{sel\ I}(\sigma)$	$\langle\Delta\theta\rangle_{sel\ II}(\sigma)$
3C324	2.0	0.208	0.64(0.39)	1.27(0.28)	1.36(0.39)
Q2237+0305	1.8	0.949	1.23(0.68)	1.77(0.68)	2.41(0.81)
Q0142-100	2.2	0.609	1.89(1.15)	2.32(1.01)	3.02(0.97)
MG1654+134	2.1	0.800	2.48(1.52)	2.87(1.37)	3.57(1.27)
H1413+117	1.1	0.240	0.74(0.46)	1.35(0.35)	1.53(0.46)

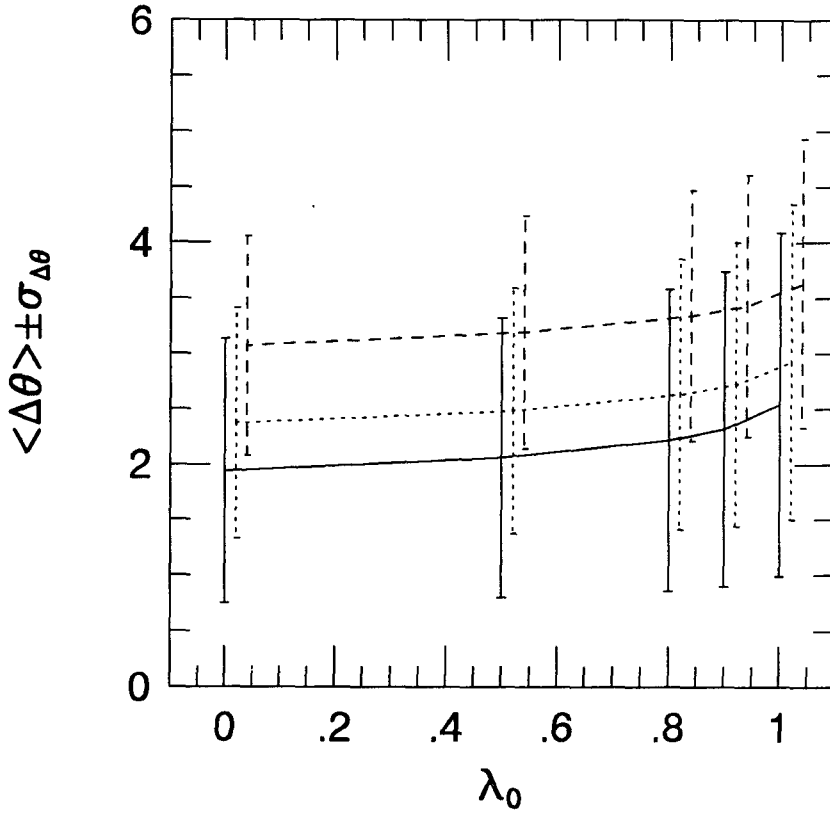


Fig. 2. Graph of $\langle\Delta\theta\rangle$ and $\sigma_{\Delta\theta}$ vs. λ_0 for Q0142 - 100.
 No selection effect is denoted by solid line, selection effect I by dotted line, selection effect II by dashed line.
 Error bars represent $\sigma_{\Delta\theta}$ and are shifted for clarity.

models that can be rejected with 95% confidence. Only the model (A) with the selection effect I can be rejected with 90 % confidence.

However, chi-square test is based on the normal distribution and because the probability distribution of image separation does not follow the normal distribution(see e.g., Figure 3), we need to use more suitable statistical analysis.

iii) The probability distribution of the angular separation and likelihood test

The calculated probability distribution, $dP_i/d\Delta\theta$, for each pair of z_L and z_S -same as those of observed lens systems - are shown in Figures 3 ~ 7. The distribution in case of no selection effect is denoted by solid line, selection effect I by dotted line, selection effect II by dashed line. The arrows indicate $\Delta\theta_{obs}$, the image separation of observed lens systems.

In order to compare statistically the observed cases with the predicted distributions, we define T as likelihood,

Table 3. χ^2_ν and probability value of chi-square test $P(\chi^2_\nu, \nu)$

Model(Ω_0, λ_0)	$\chi^2_{\nu no\ sel} [P(\chi^2_\nu, \nu)]$	$\chi^2_{\nu sel I} [P(\chi^2_\nu, \nu)]$	$\chi^2_{\nu sel II} [P(\chi^2_\nu, \nu)]$
A(1.0,0.0)	3.7809 [0.01]	2.1422 [0.07]	1.7335 [0.14]
B(0.5,0.5)	2.8129 [0.02]	1.6674 [0.15]	1.4578 [0.21]
C(0.2,0.8)	1.8762 [0.11]	1.1932 [0.31]	1.3599 [0.26]
D(0.1,0.9)	1.4671 [0.21]	0.9908 [0.41]	1.3968 [0.23]
E(0.0,1.0)	0.9961 [0.41]	0.7737 [0.54]	1.6461 [0.16]
F(0.1,0.0)	3.2748 [0.01]	1.8990 [0.11]	1.5427 [0.19]

Table 4. The product of the probability ($dp_i/d\Delta\theta$) for gravitational lens systems for six cosmological models

Model(Ω_0, λ_0)	$T_{no\ sel}$	$T_{sel I}$	$T_{sel II}$
A(1.0,0.0)	8.22×10^{-5}	4.16×10^{-3}	1.19×10^{-3}
B(0.5,0.5)	2.01×10^{-4}	5.80×10^{-3}	1.12×10^{-3}
C(0.2,0.8)	4.62×10^{-4}	7.25×10^{-3}	8.10×10^{-4}
D(0.1,0.9)	6.54×10^{-4}	7.41×10^{-3}	5.71×10^{-4}
E(0.0,1.0)	8.80×10^{-4}	5.77×10^{-3}	2.02×10^{-4}
F(0.1,0.0)	1.31×10^{-4}	5.10×10^{-3}	1.24×10^{-3}

where

$$T = \prod_{i=1}^5 \frac{dP_i}{d\Delta\theta} \Big|_{obs}, \quad (30)$$

the product of the predicted probability distribution of five gravitational lens systems for given cosmological model. The results are shown in Table 4. For no selection effect, T is the greatest in the model (E). For selection effect I T is greatest in the models (C) and (D). On the other hand, for selection effect II, T is the greatest in open model (F) and the models (A) and (B), while T is smaller in the models (D) and (E) with λ_0 close to 1. Therefore, when we assume no selection effect or selection effect I, models with large λ_0 is favored. However, the same models are disfavored if we assume selection effect II.

iv) Monte-Carlo test

Though we could choose relatively more suitable cosmological model using the likelihood value, we can not assess its statistical significance. So we calculate the probability of the observed gravitational lensing event using Monte-Carlo simulation (Maoz & Rix 1993). A likelihood function L is defined as

$$L = \ln \left[\prod_i^5 \frac{dP_i}{d\Delta\theta} \Big|_{\Delta\theta_i} \right]. \quad (31)$$

A random sample of $\Delta\theta_i$ is drawn from $dP_i/d\Delta\theta$, and its L value is calculated.

$$r_i = \int_0^{\Delta\theta_i} \frac{dP_i}{d\Delta\theta'_i} d\Delta\theta'_i \quad (32)$$

This L value is compared with $L_{obs} \equiv L(\Delta\theta_i = \Delta\theta_{obs}^i)$. The number of Monte-Carlo draws in which the value of L is smaller than L_{obs} , the number in which the value of L is greater, and their percentages are shown in Table 5: if the former is small, the observed $\Delta\theta_i$ are less likely to follow the predicted probability distribution of the models. The probability that the observed angular separations of images are realized is the greatest in the model (E) with $\lambda_0 = 1.0$ in case of no selection effect or selection effect I; there is little difference between the models for selection effect II. It shows the same tendency as in §III.a.ii ~ §III.a.iii : lens systems like the observed ones are more likely in larger λ_0 model. However, none of the models considered are rejected with 95% confidence. Best we can do is

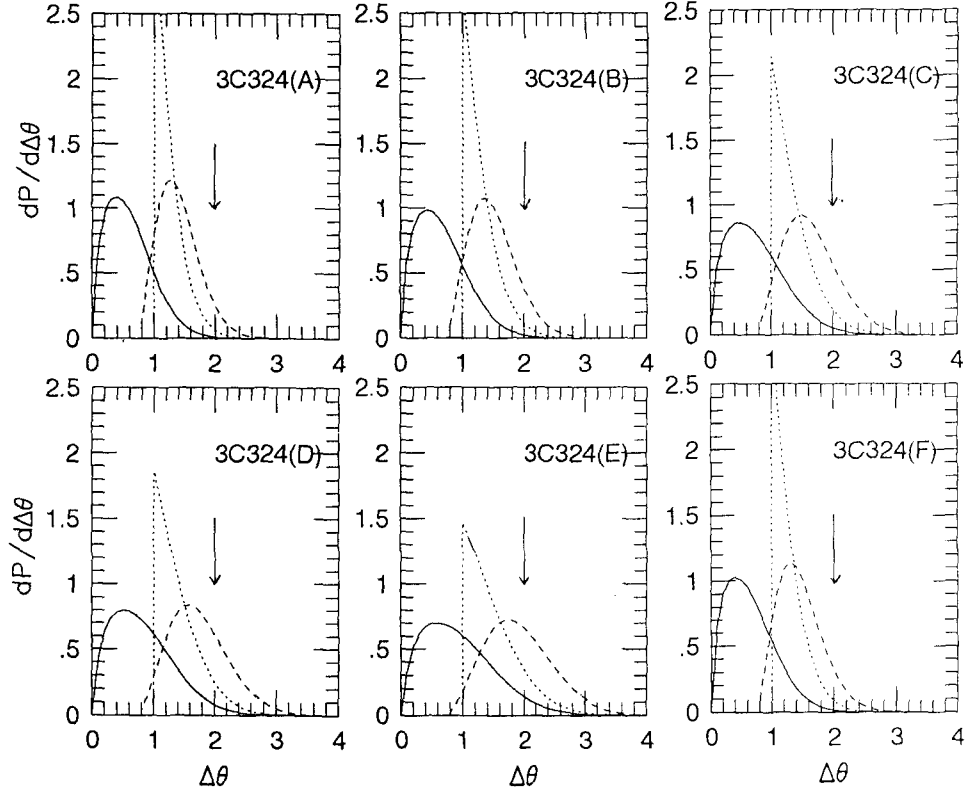


Fig. 3. Theoretically predicted $dP_i/\Delta\theta$ for gravitational lens systems with source and lens redshift same as those of 3C324 for six cosmological models.

Solid line is $dP/d\Delta\theta$ without selection effect, dotted line with selection effect I, dashed line with selection effect II. The angular separation of the lens system 3C324 is marked by the vertical arrow.

to reject the model (A) with $\lambda_0 = 0.0$ for no selection effect with 89% confidence. Although we can see the general trends, it is not yet possible to discriminate any models with any significance because of the fundamental difficulty that the number of the observed gravitational lens system is small. Thus, as more gravitational lens systems are discovered, we would be better off to exclude unsuitable models by using this method, and find the right one.

(b) Discussions

The uncertainties in our analyses need to be carefully studied because we simplified the complex lensing statistics. So we discuss two of the most important ones.

i) Angular selection effect

In §III.a, we see that, although the general trend of the test is same, details become dependent on the form of the angular selection function. Among the three forms of selection effect, we believe selection effect I better describes the actual observational situations: It is yet difficult to find lens systems with separation below $1.0''$ from ground, albeit the steady improvement of angular resolution. On the other hand, selection effect II underestimates the angular resolution of recent observations (Kochanek 1993, Park 1994). So we argue that the cosmological models with large λ_0 is relatively more consistent with the observations.

ii) Dependence on observation sample

Judging whether a specific case is a genuine gravitational lens system can be confusing at times. So to see the effect due to the sample selection, we adopt the same method as in §III.a.iii to the sample of the gravitational lens

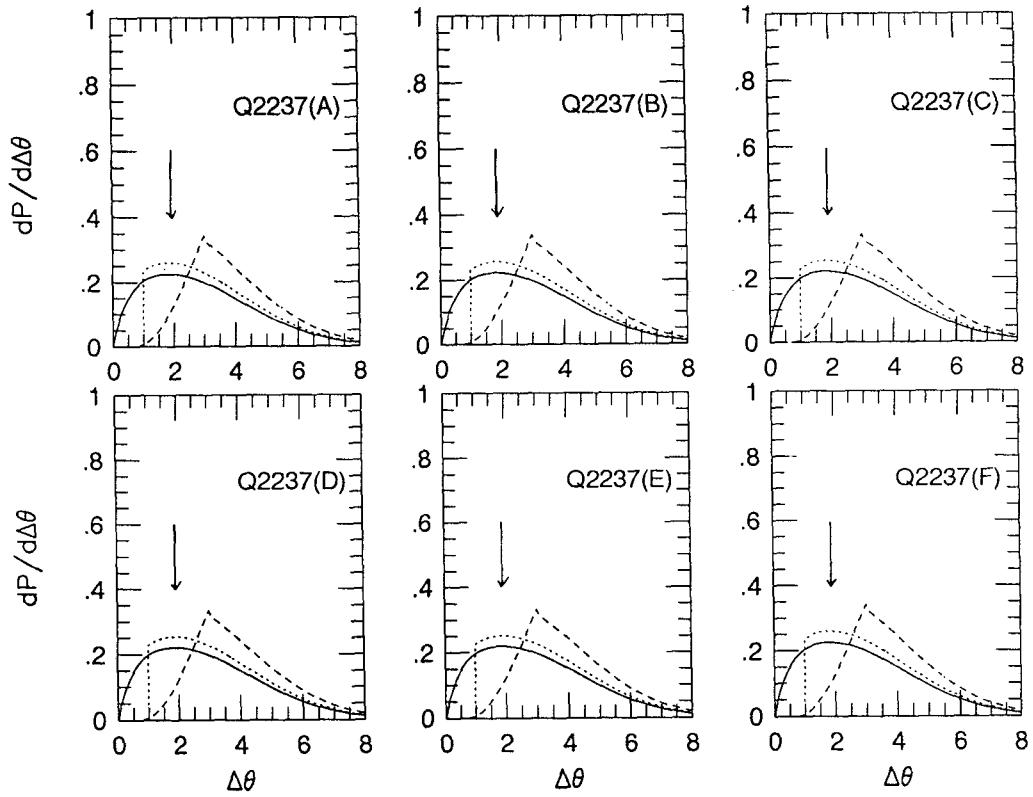


Fig. 4. Same as Fig. 3. for Q2237+030

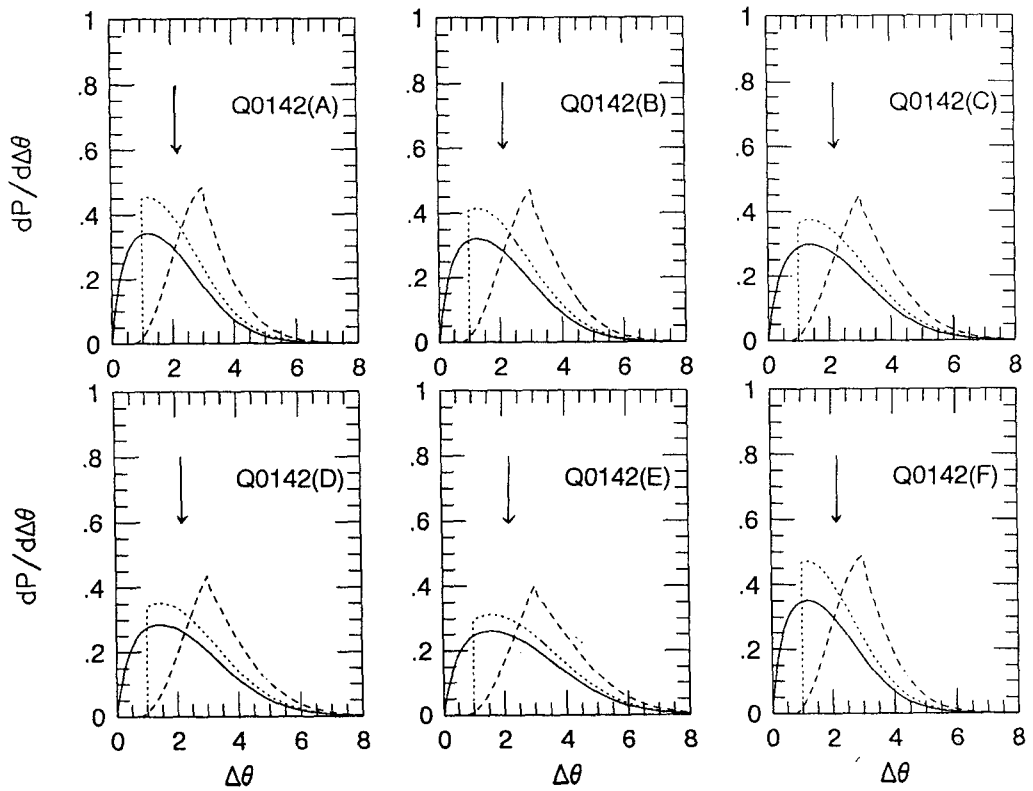


Fig. 5. Same as Fig. 3. for Q0142-100

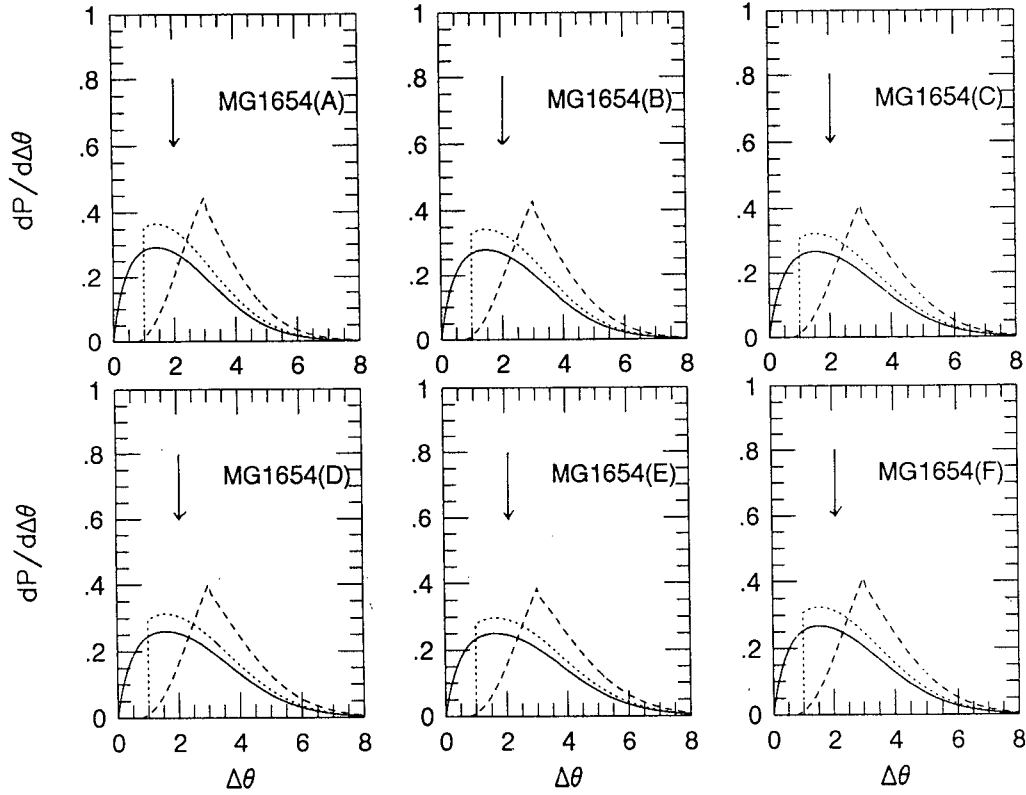


Fig. 6. Same as Fig. 3. for MG1654+134

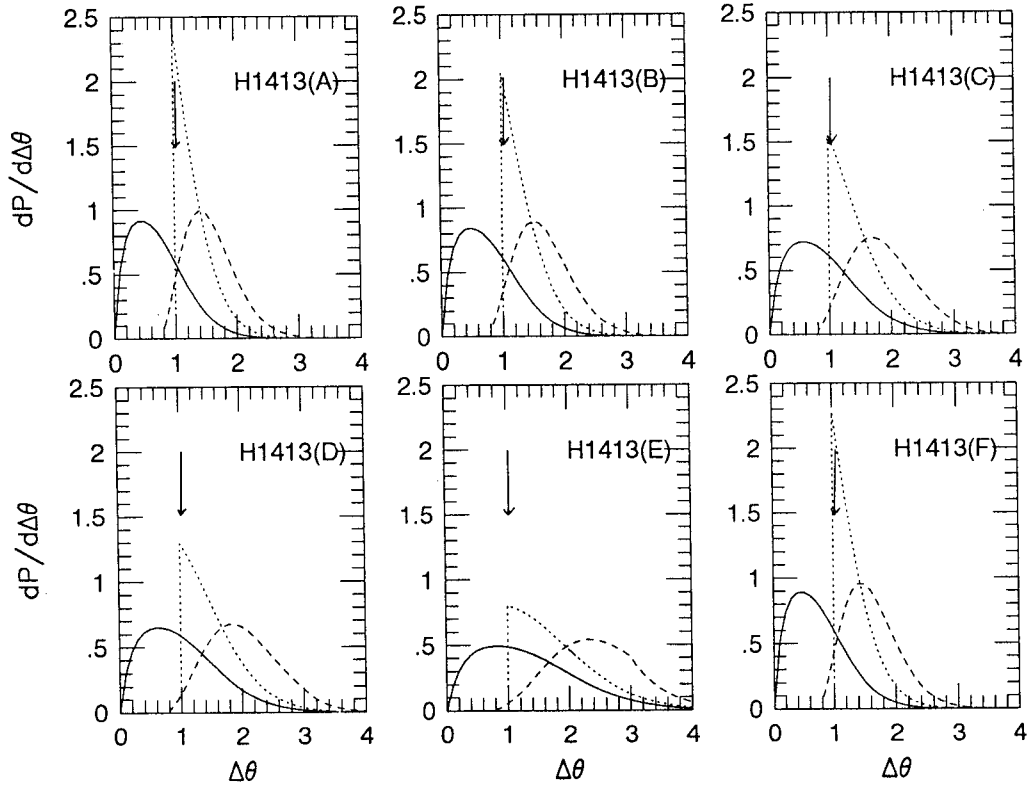


Fig. 7. Same as Fig. 3. for H1413+117

Table 5. Result of Monte-Carlo simulation:
The numbers of simulated cases having likelihood
smaller/larger the observed systems are listed.

$Model(\Omega_0, \lambda_0)$	no sel(smaller:larger)(%)	sel I (smaller:larger)(%)	sel II (smaller:larger)(%)
A(1.0,0.0)	556:4444(11/89)	1103:3897(22/78)	1121:3879(22/78)
B(0.5,0.5)	753:4247(15/85)	1350:3650(27/73)	1201:3791(24/76)
C(0.2,0.8)	1052:3948(21/79)	1678:3322(34/66)	1254:3746(25/75)
D(0.1,0.9)	814:4183(16/84)	1866:3134(37/63)	1221:3779(24/76)
E(0.0,1.0)	1722:3728(34/66)	2168:2832(43/57)	1039:3961(21/79)
F(0.1,0.0)	646:4354(13/87)	1128:3772(25/75)	1181:3819(24/76)

systems different from those of §III.a: We leave out the uncertain case, 3C324 whose z_L is not accurately known. With the new sample, T of the model (B) with $\lambda_0 = 0.5$ is the greatest for no selection effect, and for selection effect I and II, T of the model (A) with $\lambda_0 = 0.0$ is the greatest. This shows that the result of the analysis can depend on which gravitational lens systems are selected for comparison. Though no model is rejected with high confidence, therefore no statistically significant contradiction, we have to be very careful in applying these analyses: one wrong case can invalidate the conclusion. Definitely, more data is needed for this kind of statistical test to be robust.

iii) Dependence on statistical method

There are quite a few more sources of uncertainties: deviation from spherical symmetry, possibility of aiding by undetected cluster, effect of other galaxies near the line of sight and so forth. Some of them will be the subject of future study.

IV. Conclusions

We calculate and compare the predicted distribution of angular separation of images with that of the observed angular separations in multiple image gravitational lens systems using a variety of statistical analyses. Lensing galaxies are modeled as singular isothermal spheres and angular selection effects in observations are considered by three simple functions. We use generic chi-square test, likelihood test, and Monte-Carlo test to reject or find the cosmological model, most or least consistent with observation. Though there are some uncertainties, the flat model with large cosmological constant is more compatible with the observation: they produce larger image separations as seen in data. However, no model is strongly (95% confidence) rejected due to the small number of observed multiple image lens systems. This result shows a different tendency from that of Fukugita et al.'s (1992), who compared the probability of multiple image gravitational lensing event with the number of the observed gravitational lens systems: the model with λ_0 greater than 0.9 is rejected because too many lens systems are expected in that model.

Although, this kind of test is not robust or strong enough to discriminate with certainty among various flat cosmological models at present, the large scale observations like Sloan Digital Sky Survey will produce enough gravitational lens systems to pick out the correct cosmological model.

REFERENCES

- Boyle, B. J., Frog, R., Shanks, T., Peterson, B. A., 1990, MNRAS, 234, 1
 Carroll, W. M., Press, W. H., Turner, E. L., 1992, Ann. Rev. Ast. Aphys., 30, 499
 Faber, S. M., Jackson, R. E., 1976, ApJ, 204, 688
 Fukugita, M., Futamase, M., Kasai, M., Turner, E. L., 1992, ApJ, 393, 3 (FFKT)
 Fukugita, M., Turner, D. L., 1991, MNRAS, 253, 99 (FT)
 Gott, J. R., Park, M. G., Lee, H. M., 1989, ApJ, 338, 1 (GPL)
 Herwitt, A., Burbidge, G., 1987, ApJS, 63, 1

- Herwitt, A., Burbidge, G., 1989, ApJS, 69, 1
Kochanek, 1993, ApJ, 417, 438
Koo, D. C., & Kron, R. G., 1992, Ann. Rev. Ast. Aphys., 30, 613
Maoz, D., Rix, H. W., 1993, ApJ, 416, 425
Park, 1994, preprint
Tully, R. B., Fisher, J. R., 1977, A&A, 54, 661
Turner, E. L., Ostriker, F. P., Gott, J. R., 1984, ApJ, 284, 1 (TOG)
Walsh, D., Carswell, R. F., Weymann, R. J., 1979, Nature, 279, 381
Young, P., Gunn, J.E., Oke, K. T., Westphal, J. A., 1980, ApJ, 241, 507
Weinberg, S., 1972, Gravitation and Cosmology, (Willey : New York)